Cestode larvae excite host neuronal circuits via glutamatergic signaling.

Anja de Lange[*1,2,3], Hayley Tomes[*1,2,3], Joshua S Selfe[1,2,3], Ulrich Fabien Prodjinotho[4], Matthijs B Verhoog[1,2], Siddhartha Mahanty[5], Katherine Smith[3,6], William Horsnell[3,7,8], Chummy Sikasunge[9], Clarissa Prazeres da Costa[4], Joseph V Raimondo[1,2,3]

[*]Authors contributed equally

[1]Division of Cell Biology, Department of Human Biology, Faculty of Health Sciences, University of Cape Town, Cape Town, South Africa
[2]Neuroscience Institute, Faculty of Health Sciences, University of Cape Town, Cape Town, South Africa
[3]Institute of Infectious Disease and Molecular Medicine, Faculty of Health Sciences, University of Cape Town, Cape Town, South Africa
[4]Center for Global Health, TUM School of Medicine, Technical University of Munich (TUM), Munich, Germany
[5]Department of Medicine, The Peter Doherty Institute for Infection and Immunity and the Victorian Infectious Diseases Service, University of Melbourne, Melbourne, Australia
[6]School of Biosciences, Cardiff University, Cardiff, United Kingdom
[7]Institute of Microbiology and Infection, University of Birmingham, Birmingham, United Kingdom
[8]Laboratory of Experimental and Molecular Immunology and Neurogenetics (INEM), UMR 7355 CNRS-University of Orleans, Orleans, France
[9]School of Veterinary Medicine, Department of Paraclinicals, University of Zambia, Lusaka, Zambia

Correspondence:
Joseph V. Raimondo
email: joseph.raimondo@uct.ac.za

Keywords

Cestode, *Taenia crassiceps*, *Taenia solium*, neurocysticercosis, glutamate, aspartate, seizures

Abstract

Neurocysticercosis (NCC) is caused by infection of the brain by larvae of the parasitic cestode *Taenia solium*. It is the most prevalent parasitic infection of the central nervous system and one of the leading causes of adult-acquired epilepsy worldwide. However, little is known about how cestode larvae affect neurons directly. To address this, we used whole-cell patch-clamp electrophysiology and calcium imaging in rodent and human brain slices to identify direct effects of cestode larval products on neuronal activity. We found that both whole cyst homogenate and excretory/secretory products of cestode larvae have an acute excitatory effect on neurons, which can trigger seizure-like events *in*

vitro. Underlying this effect was cestode-induced neuronal depolarization, which was mediated by glutamate receptor activation but not by nicotinic acetylcholine receptors, acid-sensing ion channels nor Substance P. Glutamate-sensing fluorescent reporters (iGluSnFR) and amino acid assays revealed that the larval homogenate of the cestodes *Taenia crassiceps* and *Taenia solium* contained high concentrations of the amino acids glutamate and aspartate. Furthermore, we found that larvae of both species consistently produce and release these excitatory amino acids into their immediate environment. Our findings suggest that perturbations in glutamatergic signaling may play a role in seizure generation in NCC.

51 *Introduction*

52 Neurocysticercosis (NCC) is the most prevalent parasitic infection of the central nervous system (CNS)
53 (1,2). It is caused by the presence of larvae of the cestode *Taenia solium (T. solium)* in the brain (3).
54 The most common symptom of NCC is recurrent seizures (4). As a result, NCC is one of the leading
55 causes of adult-acquired epilepsy worldwide (5), resulting in significant morbidity and mortality. In
56 *T.solium* endemic areas, 29% of people with epilepsy also had NCC (6). Despite the impact of NCC,
57 there are a paucity of studies investigating the seizure mechanisms involved (7). As far as we are
58 aware, to date there have been no studies investigating the direct, acute effects of cestode larval
59 products on neurons. As a result, precisely how larvae perturb neuronal circuits is still relatively poorly
60 understood.

61

62 In NCC seizures may occur at any stage following initial infection (8). It is thought that inflammatory
63 processes in the brain play an important role in the development of recurrent seizures (9). Previous
64 research investigating seizure development in NCC has therefore typically focused on how the host
65 neuroinflammatory response to larvae might precipitate seizures (7,10). One study by Robinson *et al*.
66 found that production of the inflammatory molecule and neurotransmitter, Substance P, produced by
67 peritoneal larval granulomas, precipitated acute seizures (11). In addition to host-derived substances,
68 cestodes themselves are known to excrete or secrete various products that interact with host cells in
69 their vicinity. Cestode larvae-derived factors are known to modulate the activation status of
70 immunocytes such as microglia and dendritic cells (12,13). However, comparatively little is known
71 about how factors contained in, or secreted by, cestode larvae might affect neurons and neuronal
72 networks directly, including whether these may have pro-seizure effects.

73

74 To address this, we used whole-cell patch-clamp recordings and calcium imaging in rodent
75 hippocampal organotypic slice cultures and in acute human cortical brain slices to demonstrate the
76 direct effects of larval products on neuronal activity. We find that both the whole cyst homogenate

77 and the excretory/secretory (E/S) products of *Taenia crassiceps (T. crassiceps)* and *T. solium* larvae
78 have a strong, acute excitatory effect on neurons. This was sufficient to trigger seizure-like events
79 (SLEs) *in vitro*. Underlying SLE induction was larval induced neuronal depolarization, which was
80 mediated by glutamate receptor activation and not nicotinic acetylcholine receptors, acid-sensing ion
81 channels nor Substance P. Both imaging using glutamate-sensing fluorescent reporters (iGluSnFR) and
82 direct measurements using amino acid assays revealed that the homogenate and E/S products of both
83 *T. crassiceps* and *T. solium* larvae contain high levels of the excitatory amino acid glutamate and to a
84 lesser extent aspartate. Lastly, we provide evidence that larvae of both species, to varying degrees,
85 can produce and release these excitatory amino acids into their immediate environment. This suggests
86 that these parasites release amino acids that could contribute to seizure generation in NCC.

87 *Results*

88 *Taenia crassiceps homogenate excites neurons and can elicit epileptiform activity.*

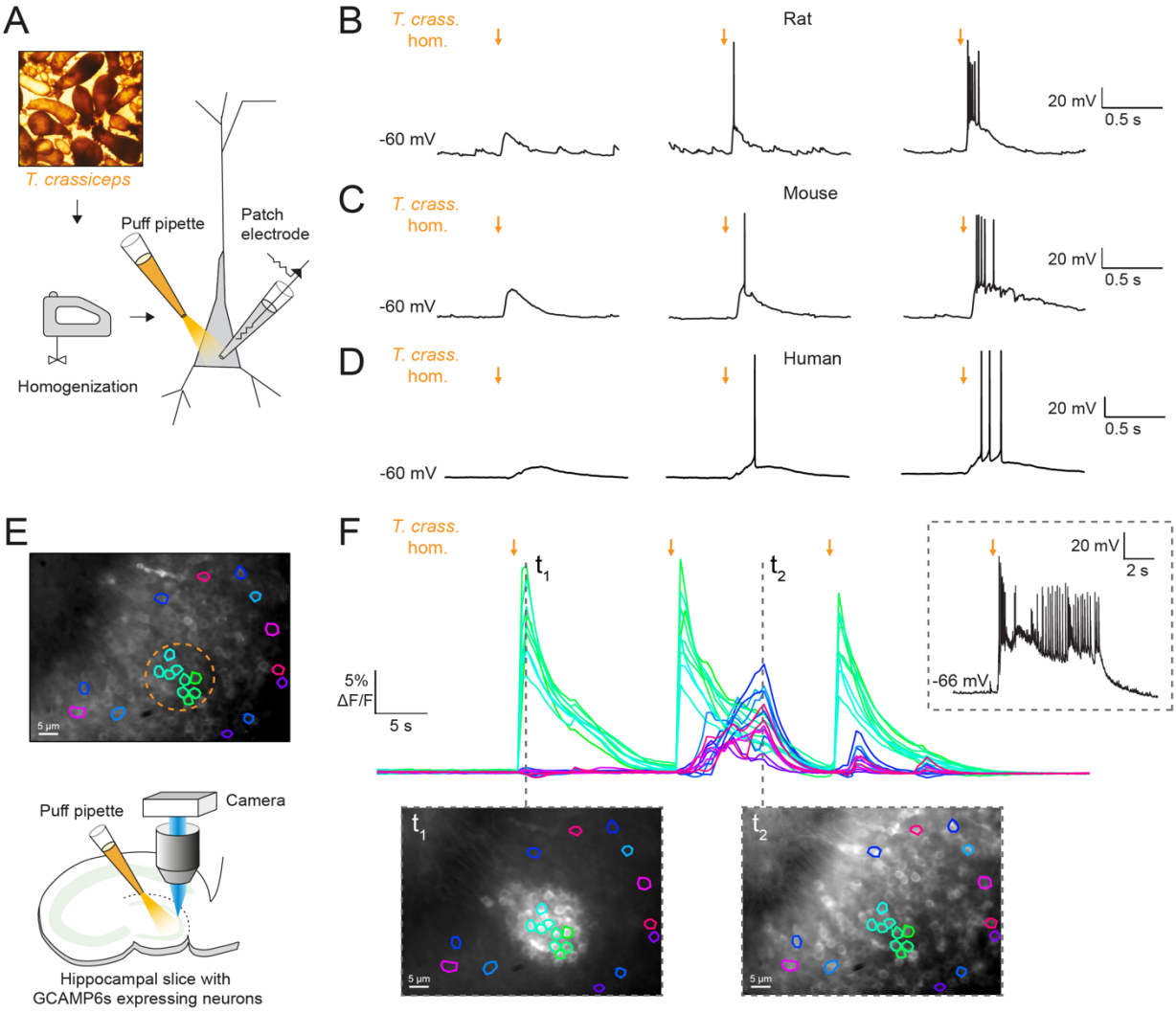

89 ***Figure 1: Taenia crassiceps homogenate excites neurons and can elicit epileptiform activity.***
90 A) Schematic showing the experimental set up in which whole-cell patch-clamp recordings were made from CA3
91 hippocampal pyramidal neurons in rodent organotypic slice cultures while a puff pipette delivered pico-litre
92 volumes of homogenised *Taenia crassiceps* larvae (*T. crass.* hom.) targeted at the cell soma. B) Current-clamp
93 recording from a rat pyramidal neuron while increasing amounts of *T. crass.* hom. was applied via the puff
94 pipette (left to right, orange arrows). Small amounts of *T. crass.* hom. resulted in depolarization (left), increasing
95 amounts by increasing the pressure applied to the ejection system elicited single (middle) or even bursts of
96 action potentials (right). C) As in 'B', identical effects of *T. crass.* hom. could be elicited in current-clamp
97 recordings from a CA3 hippocampal pyramidal neuron in a mouse organotypic brain slice culture. D) As in 'B'
98 and 'C', identical effects of *T. crass.* hom. could be elicited in current-clamp recordings from a human frontal
99 lobe layer 2/3 cortical pyramidal neuron in an acute brain slice. E) Top: widefield fluorescence image of neurons
100 in the dentate gyrus of a mouse hippocampal organotypic brain slice culture expressing the genetically encoded
101 Ca^{2+} reporter GCAMP6s under the synapsin promoter in aCSF containing 0.5 mM Mg^{2+}. A subset of neurons used
102 to generate the Ca^{2+} traces in 'E' are indicated by different colours. The orange dotted circle indicates where *T.*
103 *crass.* hom. was delivered using the puff pipette. Bottom: schematic of the experimental setup including puff
104 pipette and CCD camera for Ca^{2+} imaging using a 470 nm LED. F) Top, dF/F traces representing Ca^{2+} dynamics
105 from the GCAMP6s expressing neurons labelled in 'E' concurrent with 3 puffs (30 ms duration) of *T. crass.* hom.
106 15 s apart. Bottom: two images of raw Ca^{2+} fluorescence at two time points t_1 and t_2. Note how at time point t_2
107 neurons distant to the site of *T. crass.* hom. application are also activated, indicating spread of neuronal activity.

108 Inset, top-right: current-clamp recording from a neuron in the region of *T. crass.* hom. application demonstrates
109 seizure-like activity in response to *T. crass.* hom. application.
110
111 To investigate the potential acute effects of *T. crassiceps* larvae on neurons, *T. crassiceps* larval
112 somatic homogenate was prepared using larvae, harvested from the peritonea of mice, which were
113 freeze-thawed and homogenized (see Materials and Methods and **Fig. 1A**). Whole-cell patch-clamp
114 recordings were made from CA3 pyramidal neurons in rodent hippocampal organotypic brain slice
115 cultures and layer 2/3 pyramidal neurons in human cortical acute brain slices. Pico-litre volumes of *T.*
116 *crassiceps* homogenate were directly applied to the soma of neurons using a custom-built pressure
117 ejection system (**Fig. 1A**) (14). Application of the homogenate (20 ms puff) elicited immediate,
118 transient depolarization of the membrane voltage in recordings from rat, mouse and human neurons
119 (**Fig. 1B, C, D**). Increasing the amount of homogenate delivered by increasing the pressure applied to
120 the ejection system resulted in increasingly large membrane depolarization, which could trigger single
121 or multiple action potentials (**Fig. 1B, C, D**). To further explore the acute excitatory effect of
122 *T. crassiceps* on neurons, neuronal networks and the propagation of network activity, we performed
123 fluorescence Ca^{2+} imaging in mouse hippocampal organotypic brain slice cultures. Neurons were
124 virally transfected with the genetically encoded Ca^{2+} reporter, GCAMP6s, under the synapsin promoter
125 and imaged using widefield epifluorescence microscopy (**Fig. 1E** and Materials and Methods). To
126 simulate a pro-ictal environment, a low Mg^{2+} aCSF was used (0.5 mM Mg^{2+}) and neurons in the dentate
127 gyrus were imaged whilst small, spatially restricted puffs of *T. crassiceps* homogenate were delivered
128 every 15 s using a glass pipette (**Fig. 1E**). The cells within the direct vicinity of the puffing pipette
129 showed a sharp increase in fluorescence immediately following the delivery of *T. crassiceps*
130 homogenate (**Fig. 1F t_1**) for all 3 puffs, indicating Ca^{2+} entry following membrane depolarization and
131 action potential generation. Cells in the periphery showed notable increases in fluorescence at a
132 delayed interval following some (but not all) puffs (**Fig. 1F t_2**). The excitation of these cells are likely
133 the result of being synaptically connected to the cells that were exposed to the puff itself. Indeed, a
134 current-clamp recording from a neuron in the same slice (**Fig. 1F, inset**) indicates that a single, spatially

135 restricted puff of *T. crassiceps* homogenate can elicit the onset of a regenerative seizure-like event

136 lasting far longer than the puff itself.

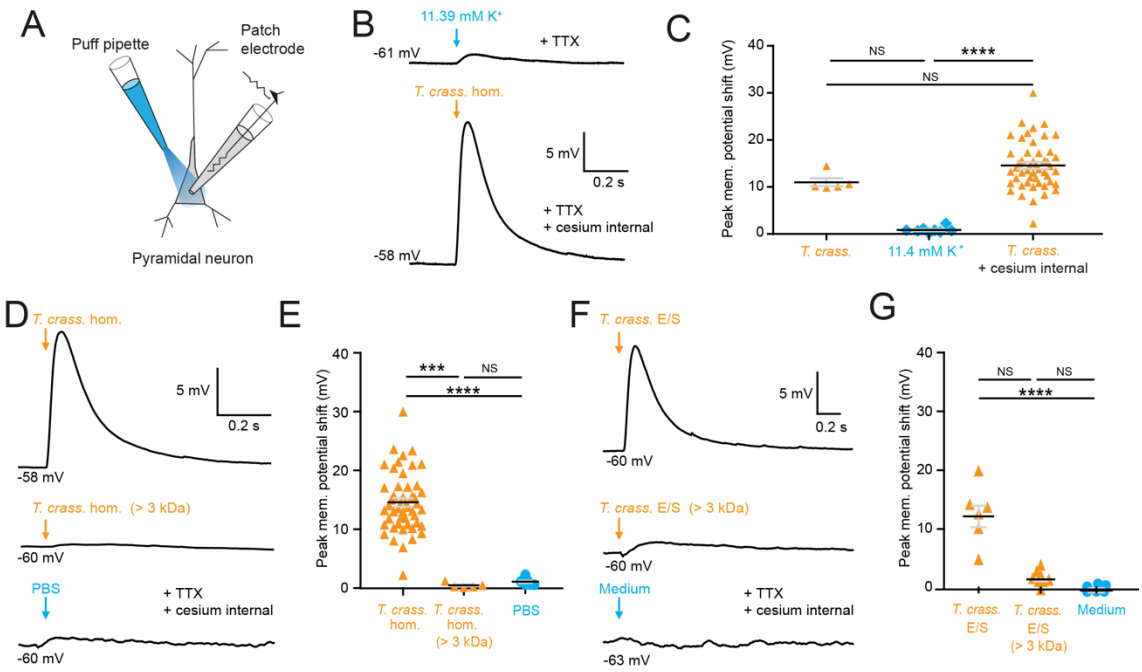

137

138 ***Figure 2: Taenia crassiceps homogenate and E/S product induced neuronal depolarization***
139 ***is mediated by a small molecule.***
140 Schematic showing the experimental set up in which whole-cell patch-clamp recordings were made from CA3
141 hippocampal pyramidal neurons in rat organotypic slice cultures while a puff pipette delivered pico-litre volumes
142 targeted at the cell soma. B) Top trace: 20 ms puff of artificial cerebrospinal fluid (aCSF) containing 11.4 mM K^+
143 (equivalent to the K^+ concentration of *T. crassiceps* homogenate (*T. crass.* hom.)) caused modest depolarization. A
144 standard internal solution was utilised, and 2 µM TTX was added to circulating aCSF to reduce synaptic noise in
145 the voltage trace. Bottom trace: 20 ms puff of *T. crass.* hom. was applied, but a cesium-based internal solution
146 was utilised to block K^+ channels in the presence of TTX. Puffs of *T. crass* hom. resulted in sizeable depolarization.
147 C) Population data showing that responses to 11.4 mM K^+ puffs were significantly smaller than that of the *T.*
148 *crass* hom. when a cesium internal solution was utilised (*T. crass*. + cesium internal), but not when a standard
149 internal solution was utilised (*T. crass*.). D) Delivery of *T. crass.* hom. caused a depolarizing shift in membrane
150 potential (top trace). The depolarizing response to *T. crass* hom. was largely abolished by dialysing out all
151 molecules smaller than 3 kDa (middle trace). PBS, the solvent for *T. crass.* hom., did not induce a large neuronal
152 depolarisation (bottom trace). E) Population data showing that the membrane depolarization induced by *T.*
153 *crass.* hom is not due to the PBS solvent and is due to a molecule smaller than 3 kDa. F) Delivery of a puff of *T.*
154 *crass* excretory/secretory (E/S) products also caused a depolarizing shift in membrane potential (top trace),
155 which was largely abolished by filtering out all molecules smaller than 3 kDa (middle trace). Culture medium,
156 the solvent for the *T. crass* E/S did not induce depolarization (bottom trace). G) Population data showing that
157 the membrane depolarization induced by *T. crass.* E/S is not due to the culture medium solvent and is due to a
158 molecule smaller than 3 kDa. Values with medians ± IQR; *** $p \leq 0.001$, ****$p \leq 0.0001$, NS = not significant.
159

160 Most cell types tend to have a high $[K^+]_i$, therefore it is conceivable that the *T. crassiceps* homogenate

161 could have a high K^+ concentration, which could potentially account for its depolarizing and excitatory

162 effects on neurons. To address this, we directly measured the ionic composition of the *T. crassiceps*

163 homogenate using a Roche Cobas 6000. The K^+ concentration of the *T. crassiceps* homogenate was

164 11.4 mM (N = 1, homogenate prepared from >100 larvae) as compared to 3.0 mM in our standard
165 aCSF (N = 1). Direct application of 11.4 mM K^+ via puff pipette during whole-cell current-clamp from
166 rat CA3 pyramidal neurons resulted in a modest median positive shift of only 0.72 mV (IQR 0.51 - 1.04
167 mV, N = 8 from 4 slices, **Fig 2B, C**) in the membrane potential, which was lower than the depolarization
168 caused by puffs of *T. crassiceps* homogenate (median 10.12 mV, IQR 9.93 - 12.49 mV, N = 5 from 4
169 slices), although this did not reach statistical significance (p = 0.26, Kruskal-Wallis test with Dunn's
170 multiple comparison test, **Fig. 2B, C**). Next, to isolate neuronal depolarization induced by *T. crassiceps*
171 homogenate, but not mediated by K^+, a cesium based internal solution was used. Despite the addition
172 of cesium the *T. crassiceps* homogenate still resulted in a large depolarisation of the membrane
173 potential (median 13.76, IQR 10.86 - 17.24 mV, N = 49 from 48 slices) which was larger than that
174 caused by 11.4 mM K^+ ($p < 0.0001$, Kruskal-Wallis test with Dunns' multiple comparison test, **Fig. 2B,**
175 **C**) but was not statistically different from that caused by *T. crassiceps* homogenate without cesium
176 internal solution (p = 0.25, Kruskal-Wallis test with Dunns' multiple comparison test, **Fig. 2B, C**).
177 Together, this indicates that although K^+ in the *T. crassiceps* homogenate may contribute to
178 membrane depolarization, much of the effect is mediated by a different component.
179
180 To determine the fraction of the *T. crassiceps* homogenate which underlies the acute excitatory effect
181 on neurons we observed, we used a dialysis membrane to separate the fraction of the homogenate
182 bigger than 3 kDa from the total homogenate. This removed molecules smaller than 3 kDa from the
183 homogenate. When this dialysed *T. crassiceps* was puffed onto the cells the depolarizing response was
184 greatly reduced. . The median positive shift in membrane potential for dialysed *T. crassiceps*
185 homogenate was only 0.27 mV (IQR 0.20 - 0.85 mV, N = 5 from 4 slices) as compared to a median for
186 the total homogenate which was 13.76 mV (IQR 10.87 - 17.24 mV, N = 49 from 48 slices, p = 0.0002,
187 Kruskal-Wallis test with Dunn's multiple comparison test, **Fig. 2D, E**). Phosphate buffered saline (PBS),
188 the solvent for the homogenate also did not produce substantial depolarisation (median 1.00 mV, IQR
189 0.58 - 1.56 mV, N = 8 from 2 slices,) when compared to the dialysed *T. crassiceps* homogenate (p >

190 0.10, Kruskal-Wallis test with Dunn's multiple comparison test, **Fig 2D, E**). This suggests that the
191 excitatory component of the *T. crassiceps* homogenate is a molecule smaller than 3 kDa.
192
193 Given that helminths are well known to excrete or secrete (E/S) products into their immediate
194 environment, we next sought to determine whether the <3kDa small molecule/s from *T. crassiceps*
195 homogenate, which was found to induce neuronal depolarisation, was also produced as an E/S
196 product by *T. crassiceps* larvae. The media was collected over a period of 21 days and either used
197 unaltered (*T. crassiceps* total E/S products) or buffer exchanged into a > 3 kDa fraction using an Amicon
198 stirred cell. Brief application of total *T. crassiceps* E/S products using a soma directed puff was
199 sufficient to cause neuronal depolarization (median 12.40 mV, IQR 9.94 - 14.07 mV,, N = 7 from 3
200 slices) significantly larger than that of the media control (median -0.61 mV, IQR –0.80 - 0.35 mV, N =
201 7 from 2 slices, p ≤ 0.0001, Kruskal-Wallis test with Dunn's multiple comparison test, **Fig. 2F, G**).
202 However, the *T. crassiceps* E/S product fraction larger than 3 kDa (median 1.25 mV, IQR 1.02 - 2.21
203 mV, N = 8 from 1 slice) did not generate significant neuronal depolarization as compared to media
204 control (p = 0.17, Kruskal-Wallis test with Dunn's multiple comparison test, **Fig. 2F, G**). Together this
205 set of experiments demonstrated that both *T. crassiceps* homogenate and T. *crassiceps* E/S products
206 contain an excitatory component, which is a small molecule.
207
208 *The excitatory effects of Taenia crassiceps are mediated by glutamate receptor activation.*
209 Robinson *et al* (2012) have found Substance P, an abundant neuropeptide and neurotransmitter, in
210 close vicinity to human NCC granulomas (11). We therefore investigated whether Substance P could
211 elicit a similar neuronal depolarizing response to that of *T. crassiceps* homogenate. However, we
212 found that 100 µM Substance P had no acute effect on the membrane potential of CA3 hippocampal
213 pyramidal neurons (median 0.08 mV, IQR 0.01 – 0.12 mV, N = 5 from 1 slice, p = 0.0625, Wilcoxon
214 signed rank test with theoretical median, **Fig. 3A, B**).
215

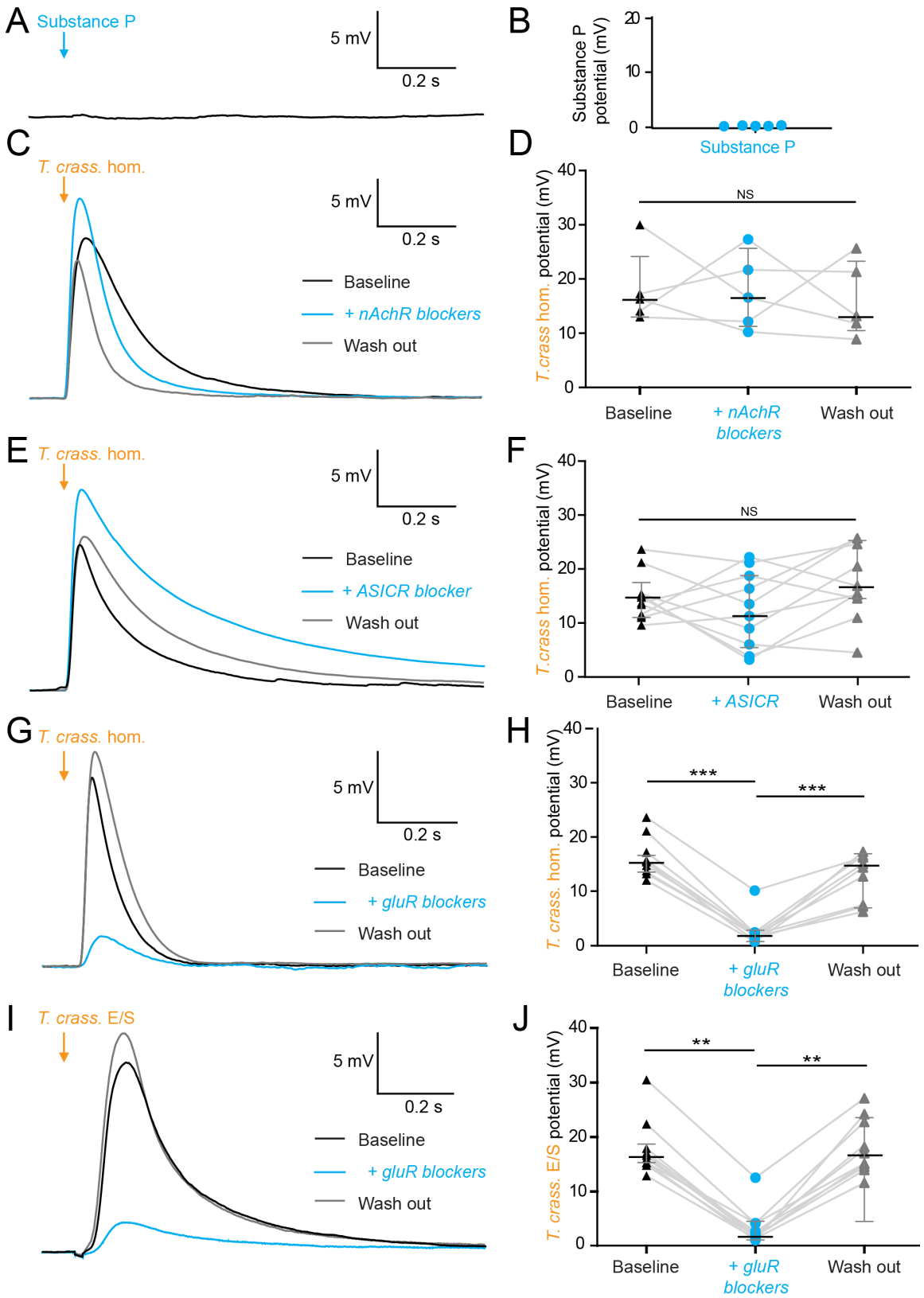

Figure 3: The excitatory effects of Taenia crassiceps are mediated by glutamate receptor activation.

Whole-cell patch-clamp recordings in current-clamp were made from CA3 pyramidal neurons in rat organotypic hippocampal slices using a cesium-based internal in the presence of 2 µM TTX. A) 20 ms puff of Substance P (100 µM) via a puff pipette directed at the soma did not affect neuronal membrane potential. B) Population data for Substance P application. C) The depolarization in response to a *T. crassiceps* homogenate (*T. crass.* hom.) puff

before (black trace), in the presence of (blue trace), and following wash out (grey trace), of a nicotinic acetylcholine receptor (nAchR) blocker (mecamylamine hydrochloride, 10 µM). D) Population data demonstrating that nAchR blockade has no significant effect on *T. crass.* hom. induced depolarization, NS = not significant. E) The depolarization in response to a *T. crass* hom. puff before (black trace), in the presence of (blue trace), and following washout (grey trace), of an ASIC receptor blocker (amiloride, 2 mM). F) Population data demonstrating that ASIC receptor blockade has no significant effect on *T. crass.* hom. induced depolarization, NS = not significant. G) The depolarization in response to a *T. crass.* hom. puff before (black trace), in the presence of (blue trace), and following washout (grey trace), of a pharmacological cocktail to block glutamate receptors (10µM CNQX, 50µM D-AP5 and 2 mM kynurenic acid). H) Population data showing that the depolarization response to *T. crass.* hom. is significantly reduced in the presence of glutamate receptor blockers and returns upon wash out, ***$p \leq 0.001$. I) The depolarization in response to a puff of *T. crass* excretory/secretory (E/S) products is also markedly reduced during glutamate receptor blockade. J) Population data showing that the depolarization response to *T. crass.* hom. is significantly reduced in the presence of glutamate receptor blockers and returns upon wash out, **$p \leq 0.01$.

Next we tested whether nicotinic acetylcholine receptors (nAchRs), well described ionotropic receptors in the nervous system (15), could elicit neuronal depolarisation. However, we found that blockade of nAchRs with mecamylamine hydrochloride (10µM) did not significantly alter the *T. crassiceps* homogenate induced depolarisation. The median *T. crassiceps* homogenate induced depolarization was 16.28 mV (IQR 13.54 - 23.63 mV) during baseline, 16.58 mV (IQR 11.21 - 24.50 mV) in the presence of mecamylamine hydrochloride and 13.20 mV (IQR = 10.37 - 23.48 mV) following washout (N = 5 from 5 slices, p = 0.6914, Friedman test, **Fig. 3C, D**). Acid-sensing ion channels (ASICs) are proton-gated sodium channels known to be expressed by hippocampal neurons and result in neuronal depolarization when activated. However, blockade of ASICs with the non-specific ASIC blocker amiloride (2 mM) did not significantly attenuate the effect of the homogenate (**Fig. 3E**), with the median *T. crassiceps* homogenate induced depolarization being 13.86 mV (IQR 11.00 – 16.48 mV) during baseline, 11.99 mV (IQR 4.97 – 19.03 mV) in the presence of amiloride, and 15.79 mV (IQR 13.25 – 24.67 mV) following washout (N = 10 from 10 slices, p = 0.1873, Friedman test, **Fig. 3E, F**).

Ionotropic glutamate receptors (GluRs) including α-amino-3-hydroxy-5-methyl-4-isoxazoleproprionic acid (AMPA), Kainate and N-methyl-D-aspartate (NMDA) receptors (16) are the major source of fast neuronal depolarisation in neurons, therefore it is likely that *T. crassiceps* homogenate could cause neuronal depolarization by activation of GluRs. To test this possibility, *T. crassiceps* homogenate-induced neuronal depolarization was measured before, during and after the application of 10µM

257 CNQX, 50µM D-AP5 and 2mM kynurenic acid (in the aCSF) to block all three classes of GluRs (all in the
258 presence of TTX and using a cesium internal solution). We found that GluR blockade significantly
259 reduced the median *T. crassiceps* homogenate induced neuronal depolarization from 14.72 mV (IQR
260 13.39 - 15.68 mV) to 1.90 mV (IQR 1.09 - 2.21 mV)), which recovered to a median value of 14.37 mV
261 (IQR 7.32 - 16.38 mV) following washout (N = 9 from 9 slices, $p \leq 0.01$, Friedman test with Dunn's
262 multiple comparison test, **Fig. 3G, H**). Similarly for *T. crassiceps* E/S products we found that application
263 of GluR antagonists reduced the median total *T. crassiceps* E/S products induced depolarization from
264 16.35 mV (IQR 15.17 - 19.03 mV) to 2.19 mV (IQR 1.67 - 4.16 mV), which recovered to a median value
265 of 16.43 mV (IQR 14.41 - 23.14 mV) following washout (N = 10 from 10 slices, $p \leq 0.01$, Friedman test
266 with Dunn's multiple comparison test, **Fig. 3I, J**). These results indicate that the acute excitatory effects
267 of both *T. crassiceps* homogenate and *T. crassiceps* E/S products are mediated through GluRs.
268
269 *Taenia crassiceps products contain excitatory amino acids detected using iGluSnFR*
270 Glutamate is the prototypical agonist of GluRs (16). We therefore sought to directly detect glutamate
271 in *T. crassiceps* larval products using glutamate-sensing fluorescent reporters. We utilized the
272 genetically encoded glutamate reporter (iGluSnFR), which was virally transfected into mouse
273 organotypic hippocampal slice cultures under the synapsin 1 gene promoter and imaged using
274 widefield epifluorescence microscopy (**Fig. 4A** and Materials and Methods). Brief puffs of *T. crassiceps*
275 homogenate delivered over the soma of iGluSnFR-expressing pyramidal neurons caused a robust
276 increase in fluorescence (median 23.32 %, IQR 5.79 – 37.66 %, N = 35 from 6 slices, **Fig. 4B, G**) when
277 compared to puffs of aCSF (median 0.0012 %, IQR -0.42 – 1.02 %, N = 12 from 1 slice, $p < 0.0001$,
278 Kruskal-Wallis test with Dunn's multiple comparison test, **Fig. 4G**). Fluorescence increases were also
279 observed with puffs of *T. crassiceps* E/S products (median 11.69 %, IQR 2.94 – 15.85 %, N = 10 from 2
280 slices, **Fig. 4C, G**) although this did not reach statistical significance when compared to puffs of aCSF
281 (median 0.0012 %, IQR -0.42 – 1.02 %, N = 12 from 1 slice, $p = 0.16$, Kruskal-Wallis test with Dunn's

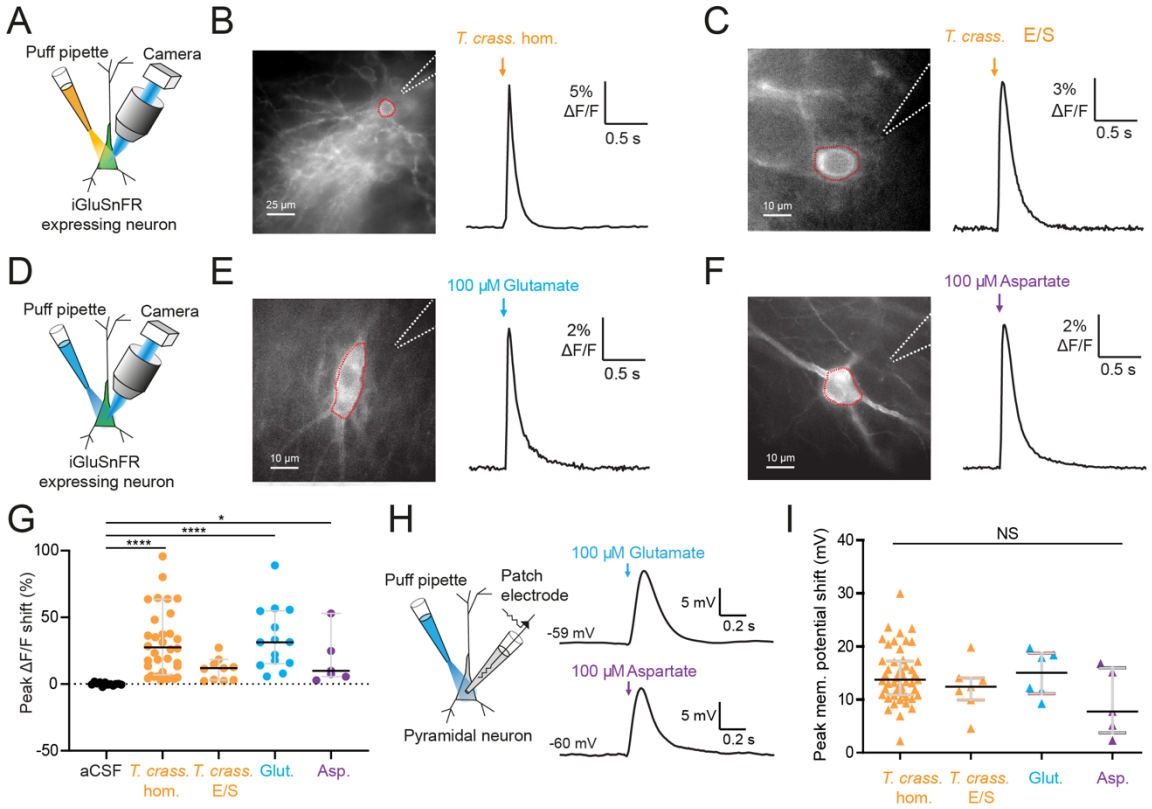

Figure 4: Taenia crassiceps products contain excitatory amino acids detected using iGluSnFR.
A) Schematic of the experimental setup for glutamate detection by the genetically encoded fluorescent glutamate reporter iGluSnFR, including puff pipette and sCMOS camera for imaging following excitation using a 475/28 nm LED-based light engine. B) Left, iGluSnFR expressing neuron with the region of interest (red dashed line) used to calculate dF/F trace (right) during a 20 ms *T. crassiceps* homogenate (*T. crass.* hom.) puff (orange arrow). C) As in 'B' but with a 20 ms *T. crassiceps* excretory/secretory (*T. crass.* E/S) product puff (orange arrow). D) Schematic of experimental setup as in 'A' but with glutamate or aspartate application via puff pipette. E) iGluSnFR fluorescence just after a 20 ms puff of aCSF containing 100 µM glutamate (blue arrow). F) As in 'E' but with iGluSnFR fluorescence during a 20 ms puff of aCSF containing 100 µM aspartate (purple arrow). G) Population data comparing peak dF/F shifts after a 20 ms puff of aCSF (as a negative control), *T. crass.* hom., *T. crass.* E/S products, aCSF containing 100 µM glutamate (as a positive control), or aCSF containing 100 µM aspartate (as a positive control), values with medians ± IQR, * $p \leq 0.05$, **** $p \leq 0.0001$. H) Schematic of whole-cell patch-clamp recording in current-clamp mode from a CA3 pyramidal neuron using a cesium-based internal and in the presence of 2 µM TTX. 20 ms puff of aCSF containing 100 µM glutamate produces a significant depolarizing shift in membrane potential (top trace), a similar puff but with 100 µM aspartate elicited a similar response (bottom trace). I) Population data comparing peak membrane potential shift after a 20 ms puff of *T. crass.* hom., *T. crass.* E/S, aCSF containing 100 µM glutamate, and aCSF containing 100 µM aspartate. Values with medians ± IQR; NS = not significant.

multiple comparison test, **Fig. 4G**). Aspartate has a similar chemical structure to glutamate and is also known to excite neurons via glutamate receptor activation (17). iGluSnFR is also known to be sensitive to aspartate as well as glutamate (18). We found that puffing aCSF containing 100 µM glutamate (median 31.35 %, IQR 15.35 – 54.92 %, N = 14 from 2 slices, **Fig. 4E, G**) or 100 µM aspartate (median 15.09 %, IQR 11.12 – 33.12 %, N = 5 from 1 slice, **Fig. 4F, G**) onto hippocampal pyramidal neurons

306 expressing iGluSnFR resulted in a significantly higher fluorescence as compared to aCSF (median
307 0.0012 %, IQR -0.42 – 1.02 %, N = 12 from 1 slice, Kruskal-Wallis test with Dunn's multiple comparison
308 test, $p \leq 0.05$, **Fig. 4G**). Similarly, puffing aCSF containing 100 µM glutamate (median 15.05 mV, IQR
309 11.12 – 18.71 mV, N = 6 from 1 slice, **Fig. 4H, I**) or 80 µM aspartate (median 7.75 mV, IQR 3.74 – 15.99
310 mV, N = 5 from 1 slice, **Fig. 4H, I**) during whole-cell current-clamp recordings elicited membrane
311 depolarizations which were similar those observed with *T. crassiceps* homogenate (median 13.76 mV,
312 IQR 10.87 – 17.24 mV, N = 49 from 48 slices, **Fig. 4I**) and E/S products (median 12.40 mV, IQR 9.94 –
313 14.07 mV, N = 7 from 3 slices, Kruskal-Wallis test with Dunn's multiple comparison test, $p > 0.05$, **Fig.**
314 **4I**).
315
316 *Taenia crassiceps larvae contain and produce glutamate and aspartate*
317 Given the short-term responses to homogenate and E/S products we observed using iGluSnFR, we
318 next sought to record possible evidence of changes in ambient glutamate or aspartate using a more
319 naturalistic setting where iGluSnFR-expressing neurons were placed adjacent to a live *T. crassiceps*
320 larva (see Materials and Methods, **Fig. 5A-C**). During imaging periods lasting up to 15 minutes,
321 fluorescence was stable, indicating no detectable oscillatory changes in ambient glutamate/aspartate
322 on the timescales recorded (N = 2 slices, **Fig. 5B, C**). Our submerged recording setup might have led
323 to swift diffusion or washout of released glutamate, possibly explaining the lack of observable
324 changes. We then directly measured the concentration of glutamate and aspartate in our *T. crassiceps*
325 products using separate glutamate and aspartate assays (see Materials and Methods). We found that
326 the median concentration of glutamate in the *T. crassiceps* homogenate and E/S products were 119.9
327 µM (IQR 73.41 – 153.2 µM, N = 5, **Fig. 5D**) and 72.32 µM (IQR 32.95 – 116.0 µM, N = 6, $p = 0.1061$,
328 Mann-Whitney test, **Fig. 5D**), respectively. The median concentration of aspartate in *T. crassiceps*
329 homogenate and E/S products were 25.8 µM (IQR 16.5 – 35.1 µM, N = 3, **Fig. 5E**) and 44.03 µM (IQR
330 17.56 – 84.74 µM, N = 3, $p = 0.4000$, Mann-Whitney test, **Fig. 5E**), respectively. Together, these

331 findings suggest that *T. crassiceps* larval homogenate and E/S products contain the excitatory amino

332 acids glutamate and aspartate at concentrations that are sufficient to elicit neuronal depolarization.

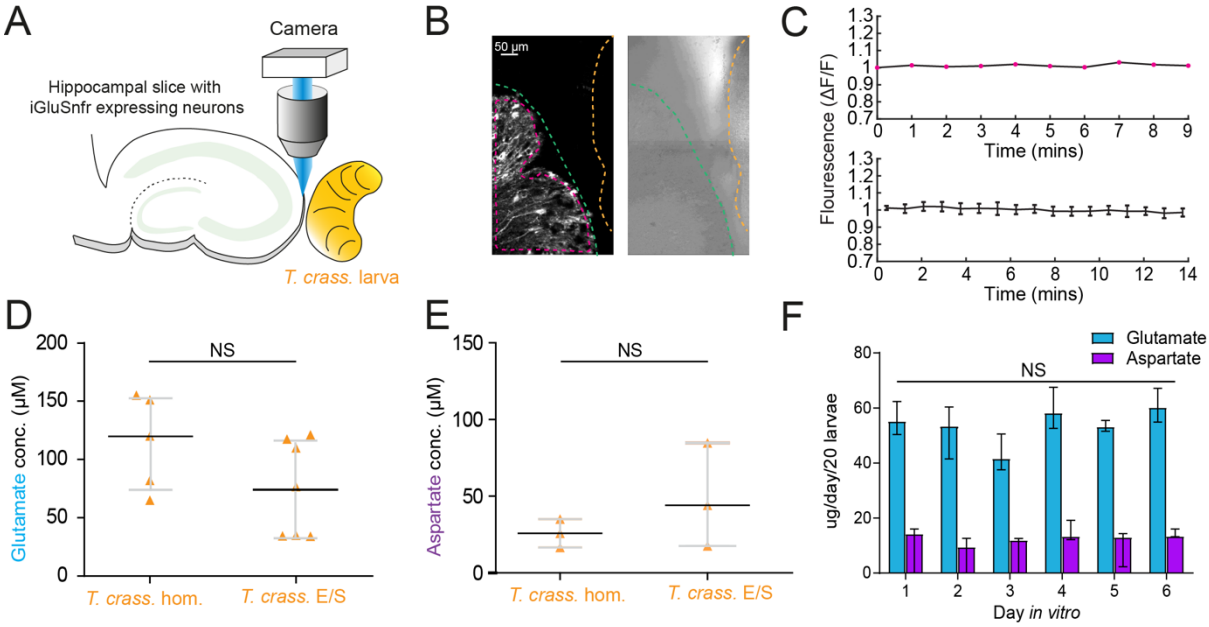

333

334 ***Figure 5: Taenia crassiceps larvae contain and produce glutamate and aspartate.***
335 A) Schematic of the experimental setup whereby a living *Taenia crassiceps* (*T. crass.)* larva is placed in close proximity
336 to a hippocampal organotypic brain slice with iGluSnFR-expressing neurons, for detection of glutamate fluctuations.
337 B) Left, fluorescence image of a slice with iGluSnFR-expressing neurons (green dashed line) adjacent to a *T. crass.* larva
338 (orange dashed line), also visible in the transmitted light image (right). The region of interest (pink dashed line) was
339 used to calculate the top dF/F trace in 'C'. C) Top, dF/F trace from the example in 'B' during a 9 minute recording.
340 Lower trace: population data of the **mean ± SEM** from 5 slice-larva pairs showed no detectable oscillations or changes
341 in glutamate. D) Glutamate concentration in *T. crass.* Homogenate (*T. crass.* hom.) and *T. crass.* excretory/secretory
342 (*T. crass*. E/S) products as measured using a glutamate assay kit, values with medians ± IQR; ns = not significant. E)
343 Aspartate concentration in *T. crass.* hom. and *T. crass.* E/S as measured using an aspartate assay kit, values with
344 medians ± IQR; ns = not significant. F) Population data showing *de novo* production of glutamate and aspartate by
345 by by *T. crass* larvae for six days *in vitro*, values with medians ± IQR; NS = not significant.
346

347 Next, to determine whether *T. crassiceps* larvae actively produce and excrete/secrete glutamate

348 and/or aspartate into their environments we measured the *de novo* daily production of glutamate and

349 aspartate by larvae following harvest of live larvae. *T. crassiceps* larvae released a relatively constant

350 median daily amount of glutamate, ranging from 41.59 – 60.15 ug/20 larvae, which showed no

351 statistically significant difference across days one to six (N = 3 per day, p = 0.18, Kruskal-Wallis test,

352 **Fig. 5F**). Similarly, *T. crassiceps* larvae released a relatively constant median daily amount of aspartate,

353 ranging from 9.43 – 14.18 ug/20 larvae, which showed no statistically significant difference across

354 days one to six (N = 3 per day, p = 0.28, Kruskal-Wallis test, **Fig. 5F**).

355

356 *Taenia solium larvae depolarize human neurons via the production of glutamate*

357 *T. crassiceps*, whilst a closely related species to *T. solium*, is not the causative pathogen in humans.
358 We therefore sought to determine whether homogenate and E/S products from *T. solium* (the natural
359 pathogen in humans), also have an excitatory effect on human neurons within human brain tissue (the
360 natural host). During whole-cell patch-clamp recordings made from human layer 2/3 pyramidal cells
361 in acute cortical brain slices, pico-litre volumes of *T. solium* larval homogenate and *T. solium* larval E/S
362 products were delivered by a glass pipette. Similarly to *T. crassiceps*, both *T. solium* homogenate (**Fig.**
363 **6A**) and *T. solium* E/S product (**Fig. 6A**) caused membrane depolarization, which was sufficient to result
364 in action potential firing.
365 We then measured the glutamate and aspartate concentration of the *T. solium* homogenate and
366 *T. solium* E/S products. Significant levels of glutamate were detected in both *T. solium* homogenate
367 (46.4 µM, N = 1, **Fig. 6C**) and the *T. solium* E/S product (722 µM, N = 1, **Fig. 6C**). However, aspartate
368 was undetectable in the *T. solium* homogenate (N = 1, **Fig. 6C**) with a low concentration of aspartate
369 observed in the E/S product (15.3 µM, N = 1, **Fig. 6C**). Finally, *T. solium* larvae were observed to release
370 glutamate on the first day post-harvest (391.1 µM/20 larvae, N = 1, **Fig. 6D**) none on the 2nd and 3rd
371 day *in vitro* (N = 1 each, **Fig. 6D)**, but produced significant amounts of glutamate on days 4, 5 and 6
372 (day 4: 131.9 µM/20 larvae, N = 1; day 5: 140.6 µM/20 larvae, N = 1; day 6: 158.8 µM/20 larvae, N =
373 1, **Fig. 6D**). Aspartate was not detected on days 1 and 3 (N = 1 each, **Fig. 6D**), but was observed to be
374 released on days 2, 4, 5 and 6 (day 2: 8.4 µM/20 larvae, N = 1; day 4: 16.8 µM/20 larvae, N = 1; day 5:
375 28.1 µM/20 larvae N = 1; day 6: 31.9 µM/20 larvae, N = 1, **Fig. 6D**). These results demonstrate that *T.*
376 *solium* larvae continually release glutamate and aspartate into their immediate surroundings.

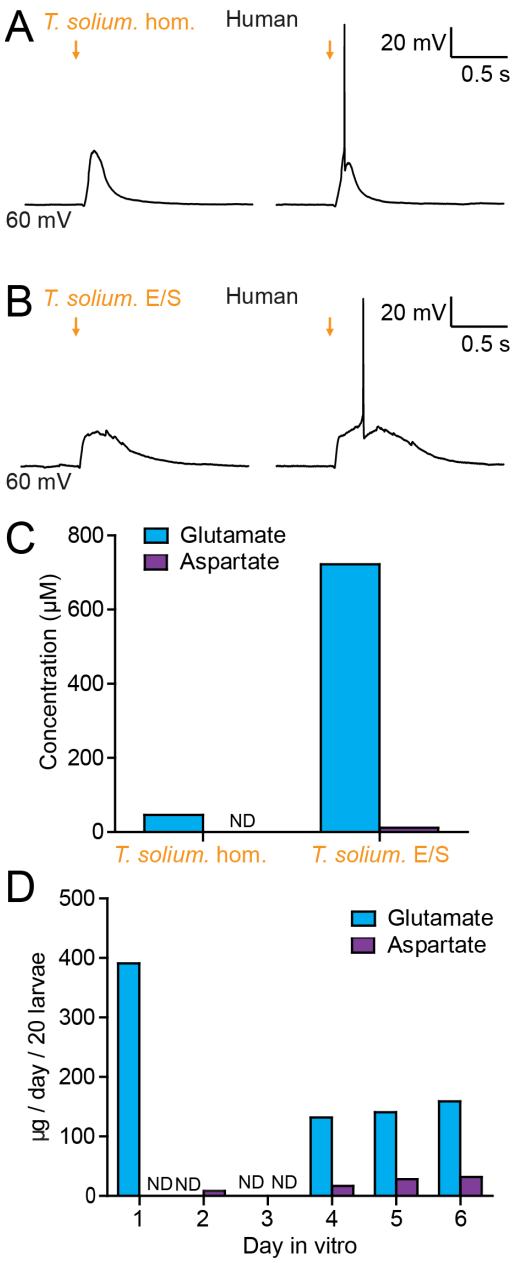

Figure 6: Taenia solium larvae depolarize human neurons via the production of glutamate.
A) Whole-cell patch-clamp recordings in current-clamp from a layer 2/3 human frontal lobe cortical pyramidal neuron in an acute brain slice, while increasing amounts of *T. solium* homogenate (*T. solium* hom.) was applied via a puff pipette (left to right, orange arrows). Small amounts of *T. solium* hom. resulted in depolarization (left), while an increased amount elicited an action potential (right). B) As in 'A', *T. solium* excretory/secretory (*T. solium* E/S) products elicited membrane depolarization and an increased amount elicited an action potential. C) Concentrations of glutamate and aspartate in *T. solium* hom. and *T. solium* E/S (N = 1, ND = not detectable). D) *De novo* production of glutamate and aspartate by *T. solium* larvae over a six day culture period (N = 1, ND = not detectable).

Discussion

Here we used patch-clamp electrophysiology, and calcium imaging in rodent hippocampal organotypic slice cultures and human acute cortical slices to demonstrate that cestode larval products cause

391 neuronal depolarization and can initiate seizure-like events via glutamate receptor activation.
392 Glutamate-sensing fluorescent reporters and amino acid assays revealed that *T. crassiceps* and
393 *T. solium* larvae contain and release the excitatory amino acid glutamate and to a lesser extent
394 aspartate.
395
396 Clinical evidence and animal models conclusively demonstrate that the presence of cestode larvae in
397 the brain can result in the generation of seizures (10,19). Previous work has focused on the
398 involvement of the host inflammatory response in seizure generation (11,20). Whilst this is likely
399 important, it does not preclude the involvement of additional or exacerbating pathogenic mechanisms
400 for seizure generation and epileptogenesis in NCC. In this study we have identified that *Taenia* larvae
401 have a direct excitatory effect on neurons via glutamatergic signaling. This is important, as the central
402 role of glutamatergic signaling in epileptogenesis has conclusively been shown using multiple cell
403 culture (21–23), slice (24–26), and *in vivo* models of epilepsy (27–29).
404
405 Clinically, in addition to NCC, the other major causes of adult acquired epilepsy are stroke, traumatic
406 brain injury and CNS tumors (30,31). In these other causes of acquired epilepsy, glutamatergic
407 signaling and glutamate excitotoxicity are thought to be central to the pathogenic process. Glutamate
408 excitotoxicity occurs when depolarized, damaged or dying neurons release glutamate, which activate
409 surrounding neurons via NMDA and AMPA receptors, resulting in sustained neuronal depolarization,
410 Ca^{2+} influx and the subsequent activation of signaling cascades and enzymes. These in turn lead to cell
411 death via necrosis and apoptosis (32), the further release of intracellular glutamate and the
412 propagation of the excitotoxic process to neighbouring cells. In the neurons that survive, the
413 prolonged exposure to glutamate has been shown to cause hyperexcitability and seizures (21,23) via
414 multiple mechanisms including enhanced intrinsic excitability and NMDA receptor dependent
415 disruption of GABAergic inhibition (33–35). Given our finding that cestode larvae contain and release
416 significant quantities of glutamate, it is possible that homeostatic mechanisms for taking up and

417 metabolizing glutamate fail to compensate for larval-derived glutamate in the extracellular space.
418 Therefore, similar glutamate-dependent excitotoxic and epileptogenic processes that occur in stroke,
419 traumatic brain injury and CNS tumors are likely to also occur in NCC.
420
421 Glioma, a common adult primary brain tumor, which typically presents with seizures in over 80% of
422 patients (36), is an intriguing condition for comparison to NCC. Here, the tumor cells themselves have
423 been shown to release glutamate into the extracellular space via the system x_c^-cystine-glutamate
424 antiporter (35). Interestingly, there is compelling evidence that tumoral release of glutamate via this
425 mechanism both causes seizures and favours glioma preservation, progression and invasion in cases
426 of malignant glioma (37–39). Analogously it is possible that *Taenia* larvae in the brain utilize the
427 release of glutamate and the induction of glutamate excitotoxicity to facilitate their growth and
428 expansion, with the accompanying effect of seizure generation. In addition, the death of *Taenia* larvae,
429 or larval-derived cells, would also result in the release of metabolic glutamate, further contributing to
430 glutamate release and excitotoxicity. In the case of glioma, where the mechanism of glutamate release
431 by tumor cells is known, pharmacological agents (*e.g.,* sulfasalazine), which block glutamate release
432 have considerable potential as therapeutic agents for reducing seizure burden in this condition.
433 Therefore, it is important that future work attempts to identify the molecular mechanisms underlying
434 the *Taenia*-specific production of glutamate to inform the development of new therapeutic strategies
435 to potentially reduce larval expansion and possibly treat seizures in NCC.
436
437 An important consideration is how we might reconcile our findings of glutamate release by *Taenia*
438 larvae with the clinical picture of delayed symptom onset in NCC. In people with NCC, some experience
439 acute seizures immediately following infection whilst others present with seizures months to years
440 following initial infection (40,41). This suggests that multiple different, or possibly interacting,
441 mechanisms might be involved in the epileptogenic process in NCC. A recent report has shown that *T.*
442 *solium* cyst products mimicking viable cysts contain the enzyme glutamate dehydrogenase, which

443 metabolizes glutamate, whilst products mimicking degenerating cysts do not (42). This predicts that
444 the glutamate levels the brain would be exposed to would be highest when a cyst dies and releases
445 its contents into its immediate surroundings. Neuroinflammation has long been thought to be central
446 to the development of seizures in NCC. In support of this, larval suppression of host inflammatory
447 responses could help explain why many patients may remain asymptomatic for years following
448 infection. Our findings are not at odds with this line of thinking when considering the effect of
449 neuroinflammation on extracellular glutamate uptake. In the healthy brain parenchymal astrocytes
450 are optimized to maintain extracellular glutamate at low concentrations (43). However, the
451 inflammatory transition of astrocytes to a reactive phenotype is known to impede their ability to
452 buffer uptake of extracellular glutamate (44). It is therefore conceivable that cyst-associated reactive
453 astrocytosis may gradually erode the ability of homeostatic mechanisms to compensate for larvae
454 derived extracellular glutamate resulting in delayed symptom onset in NCC.
455
456 There is still considerable uncertainty regarding the precise sequence of events leading to seizure
457 onset in NCC. Nonetheless our findings provide the first evidence that, as is the case with the other
458 common causes of adult-acquired epilepsy (*i.e.* stoke, traumatic brain injury and glioma), increased
459 extracellular, parasite-derived excitatory amino acids such as glutamate, and perturbed glutamatergic
460 signaling, possibly also play a role in the development of seizures in NCC.
461
462 *Materials and Methods*
463 *Ethics statement*
464 All animal handling, care and procedures were carried out in accordance with South African national
465 guidelines (South African National Standard: The care and use of animals for scientific purposes, 2008)
466 and with authorisation from the University of Cape Town Animal Ethics Committee (Protocol No: AEC
467 015/015, AEC 014/035). Ethical approval for use of human tissue was granted by the University of
468 Cape Town Human Research Ethics Committee (HREC 016/2018) according to institutional guidelines.

469

470 *Taenia maintenance and preparation of whole cyst homogenates and E/S products*

471 Larvae of *T. crassiceps* (ORF strain) were donated to us by Dr Siddhartha Mahanty (University of
472 Melbourne, Melbourne, Australia) and propagated *in vivo* by serial intraperitoneal infection of 5–8-
473 week-old female C57BL/6 mice. Every 3 months parasites were harvested by peritoneal lavage and
474 washed once in phosphate buffered saline (PBS, 1X, pH 7.4) containing penicillin (500 U/ml);
475 streptomycin (500 ug/ml); and gentamicin sulphate (1000 ug/ml) (Sigma-Aldrich), before being
476 washed a further five times in standard PBS (1X).

477 For the preparation of *T. crassiceps* whole cyst homogenate, larvae were stored immediately after
478 harvesting at -80 °C. Later the larvae were thawed (thereby lysing the cells) and suspended in PBS (1X)
479 containing a protease cocktail inhibitor (1% vol/vol, Sigma-Aldrich) at a larval:PBS ratio of 1:3. The
480 larvae were then homogenised on ice using a Polytron homogenizer (Kinematica). The resulting
481 mixture was centrifuged at 4000 rpm for 20 minutes at 4 °C. The liquid supernatant (between the
482 white floating layer and solid pellet) was collected and sterile filtered through a 0.22 µm size filter
483 (Millex-GV syringe filter, Merck). This supernatant was then aliquoted and stored at -80 °C until use.
484 To assess whether large or small molecules were responsible for the excitation of neurons, a portion
485 of the whole cyst homogenate was dialysed using a Slide-A-Lyzer™ dialysis cassette (3kDa MWCO,
486 Separations) in 2l of artificial cerebro-spinal fluid (aCSF) at 4 °C. The aCSF solution was changed twice
487 over 24 hours. To determine the ionic composition of *T. crassiceps* whole cyst homogenate a Cobas
488 6000 analyser (Roche) was used, with ion specific electrodes for K^+ and Na^+. A Mettler Toledo
489 SevenCompact™ pH meter S210 (Merck) was used to determine the pH of the homogenate.

490 For the preparation of *T. crassiceps* excretory/secretory products, after harvesting, washed larvae
491 were maintained for 14-21 days at 37 °C in 5 % CO_2 in 50 ml tissue culture flasks (approximately 7 ml
492 volume of larvae per flask) containing culture medium consisting of Earle's Balanced Salt Solution
493 (EBSS) supplemented with glucose (5.3 g/liter), Glutamax (1X), penicillin (50 U/ml), streptomycin
494 (50 ug/ml), gentamicin sulphate (100 ug/ml) and nystatin (11.4 U/ml) (Sigma-Aldrich). Culture

495 medium was replaced after 24 hours, and the original media discarded. Thereafter, culture media
496 were replaced and collected every 48-72 hours, stored at -20 °C and at the end of the culture period,
497 thawed and pooled. The pooled conditioned medium was termed total excretory/secretory products
498 (total E/S). A portion of the total E/S was aliquoted and stored at -80 °C, while another portion was
499 concentrated (about 100X) and buffer exchanged to PBS using an Amicon stirred cell with a 3 kDa
500 MWCO cellulose membrane (Sigma-Aldrich). The concentrated product contained *T. crassiceps* E/S
501 products larger in size than 3kDa (E/S > 3kDa), in PBS (1X). This was aliquoted and stored at -80 °C.
502 The fraction of the total E/S that passed through the 3kDa membrane (E/S < 3 KDa, still in medium)
503 was also retained, aliquoted and stored at -80 °C.
504 For the preparation of *T. solium* whole cyst homogenate, larvae of *T. solium* were harvested from the
505 muscles of a heavily infected, freshly slaughtered pig. After extensive washing with sterile 1X PBS,
506 *T. solium* larvae were suspended in PBS containing phenylmethyl-sulphonyl fluoride (5mM) and
507 leupeptin (2.5 µM) at a larvae:PBS ratio of 1:3. Larvae were then homogenised using a sterile handheld
508 homogenizer at 4 °C. The resulting homogenate was sonicated (4 x 60 s at 20 kHz, 1 mA, with 30 s
509 intervals) and gently stirred with a magnetic stirrer for 2 h at 4 °C. Thereafter it was centrifuged at
510 15,000 g for 60 min at 4 °C and the liquid supernatant (between the white floating layer and solid
511 pellet) was collected. The supernatant was filtered through 0.45 µm size filters (Millex-GV syringe
512 filter, Merck), aliquoted and stored at -80 °C. All *T. crassiceps* and *T. solium* larval products were
513 assessed for protein concentration using a BCA protein or Bradford's assay kit respectively.

514 For the assessment of daily glutamate and aspartate production both *T. crassiceps* and
515 *T. solium* larvae were placed into 6 well plates (+/- 20 per well, of roughly 5mm length) with 2 ml of
516 culture medium (*Taenia solium* medium: RPMI 1640 with 10 mM HEPES buffer, 100 U/ml penicillin,
517 100 µg/ml streptomycin, 0.25 µg/ml amphotericin B and 2 mM L-glutamine; *Taenia*
518 *crassiceps* medium: EBSS with 100 U/ml penicillin, 100 µg/ml streptomycin, 11.4 U/ml nystatin and 2
519 mM Glutamax). Every 24 hours 1 ml of culture medium was collected from each well, stored at -80 °C,
520 and replaced with fresh culture medium. The concentrations of glutamate and aspartate were

521 measured using a Glutamate assay kit and an Aspartate assay kit, respectively, according to the
522 supplier's instructions (Sigma-Aldrich). '*T. solium* E/S' used in human organotypic brain slice
523 electrophysiology experiments, consisted of a mixture of equal volumes of the *T. solium* medium
524 collected on D1, D2 and D3.

525

526 *Brain slice preparation*

527 Rodent hippocampal organotypic brain slices were prepared using 6-8 day old Wistar rats and C57BL/6
528 mice following the protocol originally described by Stoppini et al., (1991). Brains were extracted and
529 swiftly placed in cooled (4 °C) dissection media consisting of Earle's balanced salt solution (Sigma-
530 Aldrich); 6.1 g/L HEPES (Sigma-Aldrich); 6.6 g/L D-glucose (Sigma-Aldrich); and 5 µM sodium hydroxide
531 (Sigma-Aldrich). The hemispheres were separated, and individual hippocampi were removed and
532 immediately cut into 350 µm slices using a McIlwain tissue chopper (Mickle). Cold dissection media
533 was used to rinse the slices before placing them onto Millicell-CM membranes (Sigma-Aldrich). Slices
534 were maintained in culture medium consisting of 25 % (vol/vol) Earle's balanced salt solution (Sigma-
535 Aldrich); 49 % (vol/vol) minimum essential medium (Sigma-Aldrich); 25 % (vol/vol) heat-inactivated
536 horse serum (Sigma-Aldrich); 1 % (vol/vol) B27 (Invitrogen, Life Technologies) and 6.2 g/l D-glucose.
537 Slices were incubated in a 5 % carbon dioxide (CO_2) humidified incubator at between 35 – 37 °C.
538 Recordings were made after 6-14 days in culture.

539 For human cortical acute brain slices, brain tissue from temporal cortex was obtained from patients
540 undergoing elective neurosurgical procedures at Mediclinic Constantiaberg Hospital to treat
541 refractory epilepsy (2 patients, details below).

542

Age at surgery	**Gender**	**Reason for surgery**	**Region**	**Tissue type**	**Epilepsy Duration**
41	Female	Refractory epilepsy	Temporal Cortex	Access	2 years
4	Male	Refractory epilepsy, Malformation of	Temporal Cortex	Least abnormal	unknown

		Cortical Development			

543

544 Informed consent to use tissue for research purposes was obtained from patients or guardians prior
545 to surgery. Resected brain tissue was transported from surgery to the laboratory in an ice-cold choline-
546 based cutting solution composed of Choline Chloride (110 mM, Sigma-Aldrich); $NaHCO_3$ (26 mM,
547 Sigma-Aldrich); D-glucose (10 mM, Sigma-Aldrich); Sodium Ascorbate (11.6 mM, Sigma-Aldrich); $MgCl_2$
548 (7 mM, Sigma-Aldrich); Sodium Pyruvate (3.1 mM, Sigma-Aldrich); KCl (2.5 mM, Sigma-Aldrich);
549 NaH_2PO_4 (1.25 mM, Sigma-Aldrich); and $CaCl_2$ (0.5 mM, Sigma-Aldrich). Cutting solution was bubbled
550 with carbogen gas (95% O_2, 5% CO_2) and had an osmolality of approximately 300 mOsm. In the lab,
551 the pia mater was carefully removed, and tissue was trimmed into blocks for sectioning using a
552 Compresstome (Model VF-210-0Z, Precisionary Instruments). Slices were cut at 350 µm thickness and
553 allowed to recover for ~30 min at 34 ^{o}C in standard aCSF composed of NaCl (120 mM, Sigma-Aldrich);
554 KCl (3 mM, Sigma-Aldrich); $MgCl_2$ (2 mM, Sigma-Aldrich); $CaCl_2$ (2 mM, Sigma-Aldrich); NaH_2PO_4 (1.2
555 mM, Sigma-Aldrich); $NaHCO_3$ (23 mM, Sigma-Aldrich); and D-Glucose (11 mM, Sigma-Aldrich). The
556 aCSF was adjusted to pH 7.4 using 0.1 mM NaOH (Sigma-Aldrich), was continuously carbogenated,
557 and had an osmolality of ~300 mOsm. After recovery, slices were left for at least 1 hr at room
558 temperature before recording.

559

560 *Electrophysiology, calcium and glutamate imaging*

561 For experiments using calcium and glutamate imaging, mouse hippocampal organotypic brain slices
562 were used. For all other experiments rat hippocampal organotypic brain slices were used. A subset of
563 experiments used acute human cortical brain slices and are specified. Brain slices were transferred to
564 a submerged recording chamber on a patch-clamp rig, which was maintained at a temperature
565 between 28 and 30 °C and were continuously superfused with standard aCSF bubbled with carbogen
566 gas (95 % O_2: 5 % CO_2, Afrox) using peristaltic pumps (Watson-Marlow). The standard aCSF was
567 composed of NaCl (120 mM, Sigma-Aldrich); KCl (3 mM, Sigma-Aldrich); $MgCl_2$ (2 mM, Sigma-Aldrich);

568 $CaCl_2$ (2 mM, Sigma-Aldrich); NaH_2PO_4 (1.2 mM, Sigma-Aldrich); $NaHCO_3$ (23 mM, Sigma-Aldrich); and
569 D-Glucose (11 mM, Sigma-Aldrich) in deionized water with pH adjusted to between 7.35 and 7.40
570 using 0.1 mM NaOH (Sigma-Aldrich). Neurons in the CA3 region of the hippocampus were visualized
571 using a Zeiss Axioskop or Olympus BX51WI upright microscope using 20x or 40x water-immersion
572 objectives and targeted for recording. Micropipettes were prepared (tip resistance between 3 and 7
573 MΩ) from borosilicate glass capillaries (outer diameter 1.2 mm, inner diameter 0.69 mm, Harvard
574 Apparatus Ltd) using a horizontal puller (Sutter). Recordings were made in current-clamp mode using
575 Axopatch 200B amplifiers (Axon Instruments) and data acquired using WinWCP (University of
576 Strathclyde) or Igor (Markram Laboratory, Ecole polytechnique fédérale de Lausanne). Matlab
577 (MathWorks) was utilised for trace analysis. Basic properties of each cell were recorded (see Figure
578 supplements). Cells were excluded from analyses if the Ra was greater than 80 Ω or if the resting
579 membrane potential was above –40 mV. Two internal solutions were used: a 'standard' internal
580 solution (K-gluconate (126 mM), KCl (4 mM), HEPES (10 mM) Na_2ATP (4 mM), NaGTP (0.3 mM) and
581 Na_2-phosphocreatine (10 mM); Sigma-Aldrich) and a 'cesium' internal solution (CsOH (120 mM),
582 Gluconic acid (120 mM), HEPES (40 mM), Na_2ATP (2 mM), NaGTP (0.3 mM) and NaCl (10 mM); Sigma-
583 Aldrich). Experimental substances were puffed onto neurons using an OpenSpritzer, a custom-made
584 pressure ejection system (46). Current was injected if required to ensure a neuronal resting membrane
585 potential within 2 mV of -60 mV. In all puffing experiments each data point represents the mean peak
586 puff-induced change in membrane potential from 10 sweeps. For wash-in recordings drugs were
587 washed in for 8 mins before recordings were made. Drugs were washed out for at least 8 mins before
588 wash-out recordings were made. In some experiments tetrodotoxin (TTX) (2 µM, Sigma-Aldrich) was
589 added to the aCSF to block voltage-gated sodium channels.
590 For calcium and glutamate imaging, organotypic hippocampal mouse brain slices were virally
591 transfected with a genetically-encoded Ca^{2+} reporter (GCAMP6s under the synapsin 1 gene promoter,
592 AAV1.Syn.GCaMP6s.WPRE.SV40, Penn Vector Core) or a genetically-encoded glutamate reporter
593 (iGluSnFR under the human synapsin 1 gene promoter, pAAV.hSynapsin.SF-iGluSnFR.A184S, Addgene)

594 one day post culture using the OpenSpritzer and imaged 5 days later using an Olympus BX51WI
595 microscope, 20x water-immersion objective, CCD camera (CCE-B013-U, Mightex for the calcium
596 imaging and an Andor Zyla 4.2 for the glutamate imaging). For the calcium imaging excitation was
597 provided using a 470 nm LED (Thorlabs). For glutamate imaging, excitation was generated using a LED-
598 based light engine, 475/28 nm (Lumencor). For both imaging paradigms a Chroma 39002 EGFP filter
599 set (480/30 nm excitation filter, 505 nm dichroic, 535/40 nm emission filter) was utilised. Images were
600 collected using µManager (47). Calcium imaging data was analysed using Caltracer3 beta. Glutamate
601 imaging data was analysed using custom scripts written in Matlab.
602 For real-time imaging of glutamate signaling in neurons adjacent to a live *T. crassiceps* larva, mouse
603 hippocampal organotypic brain slices were virally transfected with a genetically
604 encoded glutamate reporter (iGluSnFR under the human synapsin 1 promoter, pAAV.hSynapsin.SF-
605 iGluSnFR.A184S) one day post culture using the OpenSpritzer. Five to six days later a brain slice would
606 be removed from the culture insert by cutting a roughly 15 mm diameter circle of the membrane out,
607 with the brain slice located in the centre of the circle. The membrane was then placed in a glass-
608 bottomed petri dish containing a drop of aCSF, with the brain slice making contact with the glass
609 bottom. At this point, a single *T. crassiceps* larvae (harvested on the same day or one day prior) of
610 approximately 1 – 2 mm in length was inserted under the membrane with a pasteur pipette and
611 carefully maneuvered until it was adjacent to one edge of the slice. A stainless-steel washer of an
612 appropriate size was then placed on top of the membrane such that it surrounded the brain slice and
613 larva, securing them in place. An additional 2 – 3 ml of carbogen-bubbled aCSF was then added to the
614 petri-dish. The petri-dish was placed in a small incubating chamber (37 °C, 5 % CO_2) in an LSM 880
615 airyscan confocal microscope (Carl Zeiss, ZEN SP 2 software). Glutamate signaling in the brain area
616 directly adjacent to the larvae was captured with a tile scan of the area every 90 sec for 15 min using
617 a 40x water-immersion lens (Zeiss) and a 488 nm laser (Zeiss). Transmitted light was also captured to
618 confirm presence and movement of the larva at the site of interest.

619 Pharmacological manipulations were performed by bath application of drugs using a perfusion system
620 (Watson-Marlow). Mecamylamine, Amiloride, D-AP5 and CNQX were purchased from Tocris.
621 Kynurenic acid and Substance P were acquired from Sigma-Aldrich.
622
623 *Data analysis and statistics*
624 Data was graphed and analysed using Matlab, ImageJ, Microsoft Excel and GraphPad Prism. All data
625 was subjected to a Shapiro-Wilk test to determine whether it was normally distributed. Normally
626 distributed populations were subjected to parametric statistical analyses, whilst skewed data was
627 assessed using non-parametric statistical analyses, these included: Mann-Whitney test; Wilcoxon
628 ranked pairs test; Kruskal Wallis one-way ANOVA with post hoc Dunn's Multiple Comparison test; and
629 Friedman test with post-hoc Dunn's Multiple Comparison test. The confidence interval for all tests
630 was set at 95%. Raw data source files are available for download from the Open Science page of the
631 Raimondo Lab website: https://raimondolab.com/2024/08/23/data-for-2023-reviewed-preprint-
632 cestode-larvae-excite-host-neuronal-circuits-via-glutamatergic-signaling/
633
634
635 *Acknowledgements*
636 We would like to acknowledge Dr Philip Fortgens (Division of Chemical Pathology, Department of
637 Pathology, University of Cape Town and National Health Laboratory Service (affiliation when the
638 analyses were done) as well as Dr James T. Butler and Dr Roger Melvill of the Epilepsy Unit,
639 Constantiaberg Mediclinic together with two anonymous patients who provided human cortical brain
640 tissue. The research leading to these results has received funding from a Royal Society Newton
641 Advanced Fellowship (NA140170) and a University of Cape Town Start-up Emerging Researcher Award
642 to JVR and grant support from the Blue Brain Project, the National Research Foundation of South
643 Africa, the FLAIR Fellowship Programme (FLR\R1\190829): a partnership between the African
644 Academy of Sciences and the Royal Society funded by the UK Government's Global Challenges
645 Research Fund, a Wellcome Trust Seed Award and a Wellcome Trust International Intermediate

Fellowship (222968/Z/21/Z). KAS was supported by a European Commission Marie Sklodowska-Curie Global Fellowship (Grant 657638, WORMTUMORS). CS, UFP and CPdC were supported by the Federal Ministry of Education and Research of Germany (BMBF), Project title: "CYSTINET-Africa" (01KA1610, Germany II). The funders had no role in study design, data collection and analysis, decision to publish, or preparation of the manuscript.

Competing interests

The authors declare that there are no competing interests relevant to this manuscript.

References

1. Diop AG, Boer HM De, Mandlhate C, Prilipko L, Meinardi H. The global campaign against epilepsy in Africa. Acta Trop. 2003;87:149–59.
2. Preux PM, Druet-Cabanac M. Epidemiology and aetiology of epilepsy in sub-Saharan Africa. Lancet Neurol. 2005 Jan;4(1):21–31.
3. Trevisan C, Mkupasi EM, Ngowi HA, Forkman B, Johansen M V. Severe seizures in pigs naturally infected with Taenia solium in Tanzania. Vet Parasitol. 2016;220:67–71.
4. Garcia HH, Del OH. Antiparasitic treatment of neurocysticercosis - The effect of cyst destruction in seizure evolution. Epilepsy & Behavior. 2017;76:158–62.
5. Nash TE, Mahanty S, Garcia HH. Neurocysticercosis-More Than a Neglected Disease. PLoS Negl Trop Dis. 2013;7(4):7–9.
6. Ndimubanzi PC, Carabin H, Budke CM, Nguyen H, Qian YJ, Rainwater E, et al. A systematic review of the frequency of neurocyticercosis with a focus on people with epilepsy. PLoS Negl Trop Dis. 2010;4(11).
7. de Lange A, Mahanty S, Raimondo J v. Model systems for investigating disease processes in neurocysticercosis. Parasitology [Internet]. 2018 Nov 15;1–10. Available from: http://www.ncbi.nlm.nih.gov/pubmed/30430955
8. Garcia HH, Del OH. Antiparasitic treatment of neurocysticercosis - The effect of cyst destruction in seizure evolution. Epilepsy & Behavior. 2017;76:158–62.
9. Vezzani A, Fujinami RS, White HS, Preux P marie, Blümcke I, Sander JW, et al. Infections, inflammation and epilepsy. Acta Neuropathol. 2016;131:211–34.
10. Nash TE, Mahanty S, Loeb J a., Theodore WH, Friedman A, Sander JW, et al. Neurocysticercosis: A natural human model of epileptogenesis. Epilepsia. 2015 Feb;56(2):177–83.
11. Robinson P, Garza A, Weinstock J, Serpa J a, Goodman JC, Eckols KT, et al. Substance P causes seizures in neurocysticercosis. PLoS Pathog [Internet]. 2012 Feb [cited 2013 Sep 11];8(2):e1002489. Available from: http://www.pubmedcentral.nih.gov/articlerender.fcgi?artid=3276565&tool=pmcentrez&rendertype=abstract
12. Sun Y, Chauhan A, Sukumaran P, Sharma J, Singh BB, Mishra BB. Inhibition of store-operated calcium entry in microglia by helminth factors: implications for immune suppression in neurocysticercosis. J Neuroinflammation. 2014 Dec 24;11(1):210.
13. Vendelova E, Camargo de Lima J, Lorenzatto KR, Monteiro KM, Mueller T, Veepaschit J, et al. Proteomic Analysis of Excretory-Secretory Products of Mesocestoides corti Metacestodes Reveals Potential Suppressors of Dendritic Cell Functions. PLoS Negl Trop Dis. 2016;10(10):1–27.

14. Forman CJ, Tomes H, Mbobo B, Burman RJ, Jacobs M, Baden T, et al. Openspritzer: an open hardware pressure ejection system for reliably delivering picolitre volumes. Sci Rep. 2017 May;7(1):2188.
15. Bear MF, Connors BW, Paradiso MA. Neuroscience: Exploring the brain. Third. Lupash E, Connolly E, Dilernia B, Williams P, editors. Philadelphia, Baltimore, New York, London, Buenos Aires, Hong Kong, Sydney, Tokyo: Lippincott Williams & Wilkins; 2007.
16. Bear MF, Connors BW, Paradiso MA. Neuroscience: Exploring the brain. Third. Lupash E, Connolly E, Dilernia B, Williams P, editors. Philadelphia, Baltimore, New York, London, Buenos Aires, Hong Kong, Sydney, Tokyo: Lippincott Williams & Wilkins; 2007.
17. Dingledine R, McBain CJ. Glutamate and Aspartate Are the Major Excitatory Transmitters in the Brain. 1999;
18. Marvin JS, Borghuis BG, Tian L, Cichon J, Harnett MT, Akerboom J, et al. An optimized fluorescent probe for visualizing glutamate neurotransmission. Nat Methods. 2013 Feb;10(2):162–70.
19. Verastegui MR, Mejia A, Clark T, Gavidia CM, Mamani J, Ccopa F, et al. Novel Rat Model for Neurocysticercosis Using Taenia solium. Am J Pathol. 2015;185(8):2259–68.
20. Stringer JL, Marks LM, White AC, Robinson P. Epileptogenic activity of granulomas associated with murine cysticercosis. Exp Neurol. 2003 Oct;183(2):532–6.
21. Sun DA, Sombati S, DeLorenzo RJ. Glutamate Injury–Induced Epileptogenesis in Hippocampal Neurons. Stroke. 2001 Oct 1;32(10):2344–50.
22. Sombati S, Delorenzo RJ. Recurrent spontaneous seizure activity in hippocampal neuronal networks in culture. J Neurophysiol. 1995 Apr;73(4):1706–11.
23. DeLorenzo R, … SPP of the, 1998 undefined. Prolonged activation of the N-methyl-d-aspartate receptor–Ca2+ transduction pathway causes spontaneous recurrent epileptiform discharges in hippocampal neurons. National Acad Sciences.
24. Anderson WW, Anderson WW, Lewis D V., Scott Swartzwelder H, Wilson WA. Magnesium-free medium activates seizure-like events in the rat hippocampal slice. Brain Res. 1986;398(1):215–9.
25. Stasheff S, Anderson W, Clark S, Science WW, 1989 undefined. NMDA antagonists differentiate epileptogenesis from seizure expression in an in vitro model. science.sciencemag.org.
26. Ziobro JM, Deshpande LS, DeLorenzo RJ. An organotypic hippocampal slice culture model of excitotoxic injury induced spontaneous recurrent epileptiform discharges. Brain Res. 2011 Jan 31;1371:110–20.
27. Croucher MJ, Bradford HF. NMDA receptor blockade inhibits glutamate-induced kindling of the rat amygdala. Brain Res. 1990;506(2):349–52.
28. Croucher MJ, Bradford HF, Sunter DC, Watkins JC. Inhibition of the development of electrical kindling of the prepyriform cortex by daily focal injections of excitatory amino acid antagonists. Eur J Pharmacol. 1988;152(1–2):29–38.
29. Rice AC, Delorenzo RJ. NMDA receptor activation during status epilepticus is required for the development of epilepsy. Brain Res. 1998;782(1–2):240–7.
30. Hauser WA, Annegers JF, Kurland LT. Prevalence of Epilepsy in Rochester, Minnesota: 1940–1980. Epilepsia. 1991 Aug;32(4):429–45.
31. Forsgren L, Beghi E, Oun A, Sillanpaa M. The epidemiology of epilepsy in Europe - a systematic review. Eur J Neurol. 2005 Apr 1;12(4):245–53.
32. Ankarcrona M, Dypbukt JM, Bonfoco E, Zhivotovsky B, Orrenius S, Lipton SA, et al. Glutamate-induced neuronal death: A succession of necrosis or apoptosis depending on mitochondrial function. Neuron. 1995 Oct 1;15(4):961–73.
33. Lee HHC, Deeb TZ, Walker JA, Davies PA, Moss SJ. NMDA receptor activity downregulates KCC2 resulting in depolarizing GABAA receptor–mediated currents. Nat Neurosci. 2011 Jun 1;14(6):736–43.
34. Terunuma M, Vargas KJ, Wilkins ME, Ramírez OA, Jaureguiberry-Bravo M, Pangalos MN, et al. Prolonged activation of NMDA receptors promotes dephosphorylation and alters postendocytic

741 sorting of GABAB receptors. Proceedings of the National Academy of Sciences. 2010 Aug
742 3;107(31):13918–23.
743 35. Buckingham SC, Campbell SL, Haas BR, Montana V, Robel S, Ogunrinu T, et al. Glutamate
744 release by primary brain tumors induces epileptic activity. Nat Med. 2011 Oct 11;17(10):1269–74.
745 36. Santosh V, Sravya P. Glioma, glutamate (SLC7A11) and seizures-a commentary. Ann Transl
746 Med. 2017 May;5(10):214.
747 37. Sontheimer H. A role for glutamate in growth and invasion of primary brain tumors. J
748 Neurochem. 2008 Apr 1;105(2):287–95.
749 38. Takano T, Lin JHC, Arcuino G, Gao Q, Yang J, Nedergaard M. Glutamate release promotes
750 growth of malignant gliomas. Nat Med. 2001 Sep;7(9):1010–5.
751 39. Huang W, Choi W, Chen Y, Zhang Q, Deng H, He W, et al. A proposed role for glutamine in
752 cancer cell growth through acid resistance. Cell Res. 2013 May 29;23(5):724–7.
753 40. Adalid-Peralta L, Arce-Sillas A, Fragoso G, Cárdenas G, Rosetti M, Casanova-Hernández D, et
754 al. Cysticerci drive dendritic cells to promote in vitro and in vivo tregs differentiation. Clin Dev
755 Immunol. 2013;2013:1–9.
756 41. Verma A, Prasad KN, Cheekatla SS, Nyati KK, Paliwal VK, Gupta RK. Immune response in
757 symptomatic and asymptomatic neurocysticercosis. Med Microbiol Immunol. 2011 Nov
758 1;200(4):255–61.
759 42. Prodjinotho UF, Gres V, Henkel F, Lacorcia M, Dandl R, Haslbeck M, et al. Helminthic
760 dehydrogenase drives PGE 2 and IL-10 production in monocytes to potentiate Treg induction . EMBO
761 Rep. 2022 May 4;23(5).
762 43. Perea G, Araque A. GLIA modulates synaptic transmission. Brain Res Revs. 2010 May;63(1–
763 2):93–102.
764 44. Seifert G, Carmignoto G. Astrocyte dysfunction in epilepsy. Brain Res Rev. 2010 May 1;63(1–
765 2):212–21.
766 45. Stoppini L, Buchs PA, Muller D. A simple method for organotypic cultures of nervous tissue. J
767 Neurosci Meth. 1991 Apr;37(2):173–182.
768 46. Forman CJ, Tomes H, Mbobo B, Baden T, Raimondo J V. Openspritzer: an open hardware
769 pressure ejection system for reliably delivering picolitre volumes. bioRxiv. 2016;093633.
770 47. Edelstein A, Amodaj N, Hoover K, Vale R, Stuurman N. Computer Control of Microscopes
771 Using µManager. In: Current Protocols in Molecular Biology. Hoboken, NJ, USA: John Wiley & Sons,
772 Inc.; 2010. p. 14.20.1-14.20.17.
773